The Incorporation of the Chaotic Dynamics of the Double Pendulum System into the Solutions of the Kadomtsev-Petviashvili-Boussinesq Equation

Dan Sui, Penglan Liu

***Abstract*—In this paper, an innovative combination of the Kadomtsev-Petviashvili (KP) equation and the Boussinesq equation gives rise to the KPB equation. Through the transformation $u = 2(\ln f)_{xx}$, its Hirota bilinear form is derived to facilitate further research. A variety of solution types are explored, including 2D solitons, breathers, lumps, and interaction solutions. Notably, the chaotic behavior of the double pendulum system is newly applied to the study of solutions to the KPB equation. By incorporating its chaotic dynamics into relevant variables, the solutions exhibit chaos-induced uncertainty and complexity, transcending simple periodicity and predictability to reflect the complexity of real-world phenomena. This enriches the understanding of the equation, builds a bridge between theoretical mathematics and physical chaos, and contributes to the accurate description and prediction in scientific and engineering applications.**

***Index Terms*—Kadomtsev-Petviashvili equation, Boussinesq equation, soliton, breather solution, lump solution, double pendulum system.**

I. Introduction

NONLINEAR partial differential equations (PDEs) are widely used to model numerous natural phenomena. In water wave propagation, their solutions can predict the shape and position of waves across time and space, thereby facilitating maritime safety and coastal engineering. In chemical reaction kinetics, the solutions characterize changes in the concentrations of reactants and products, providing guidance for reaction optimization. In fluid thermodynamics, these equations describe fluid flow states and forces, which prove valuable for industrial and aerospace design. For plasma diffusion, their solutions help illuminate plasma distribution and transport properties—knowledge critical to fusion research and space physics. Naturally, applications extend to other fields as well. Thus, studying natural phenomena through partial differential equations holds great significance.

The KP equation is an important partial differential equation in mathematics and physics used to describe the movement of nonlinear waves. Its general form is:

$$u_{xt} + 6(u^2)_{xx} + u_{xxxx} - u_{yy} = 0, \tag{1}$$

where $u = u(x, y, t)$ is a scalar function, with x and y representing the longitudinal and transverse spatial coordinates, respectively. Let us briefly explain the meaning of each term. The term u_{xt} can be interpreted as the temporal variation of the gradient of the physical quantity u (e.g., temperature, concentration, velocity, etc.) in the x-direction. This is crucial for studying how the propagation and spatial distribution of u evolve over time. In the term $(u^2)_{xx}$, u^2 is often related to the energy or power of that physical quantity, $(u^2)_{xx}$ describes the spatial variation of energy or related physical quantities. In the context of water wave problems, it reflects the nonlinear dispersion effect, specifically the variation in propagation speed among waves of different frequencies arising from nonlinear interactions during propagation. This nonlinear dispersion effect induces changes in wave shape and gives rise to phenomena such as wave splitting or fusion during propagation.

The term u_{xxxx} is the fourth-order partial derivative of the function u with respect to the spatial variable x. Physically, it represents the high-order term in the dispersion effect of waves. The high-order spatial derivative term reflects the high-order dispersion characteristics of waves during spatial propagation. Specifically, the difference in propagation speed between waves of different frequencies in space depends not only on the first-order spatial derivative term but also on the high-order spatial derivative term. In certain cases, the presence of this term allows the equation to describe more complex wave propagation phenomena, such as wave attenuation and scattering.

The term u_{yy} can describe the diffusive or wave-like properties of the physical quantity in the y-direction. For instance, in fluid mechanics, if u represents the y-component of fluid velocity, this term can reflect how the non-uniformity of velocity in the y-direction self-adjusts (e.g., in a viscous fluid, the second derivative of velocity is associated with viscous force). Alternatively, in wave problems, it may relate to the propagation and deformation of waves along the y-direction.

In general, the KP equation comprehensively incorporates factors such as the temporal evolution, nonlinear interactions, dispersive effects, and transverse variations of waves, enabling it to accurately describe a wide range of propagation phenomena involving nonlinear waves. It finds important applications in fields including fluid mechanics, plasma physics, and nonlinear optics. The KP equation has long remained a frontier of research interest in the scientific community. Recently, Lan [16] derived its bilinear form by leveraging Bell polynomials, and subsequently constructed N-soliton solutions successfully using the Hirota method—making a notable contribution to the study of this equation.

Manuscript received March 20, 2025; revised August 1, 2025.

Dan Sui is a professor of the School of Computer and Information Engineering, Anyang Normal University, Anyang, 455000, China (e-mail:suidan128@163.com).

Penglan Liu is a postgraduate student of the Graduate School, Beijing Normal-Hong Kong Baptist University, Zhuhai, 519087, China (e-mail:lpl010507@163.com).

Furthermore, in the research paper [14], a significant milestone was reached with the first construction of positive multi-complexiton solutions to the generalized KP equation, thereby opening new avenues for further exploration and analysis of related phenomena. Ahmad et al. [2] adopted an innovative approach by employing the improved ϕ^6-model expansion method, leading to the discovery of novel solutions for the new (3+1)-dimensional integrable KP equation. Their work has introduced fresh perspectives and insights into the existing body of knowledge on the KP equation. Naturally, the literature on the KP equation is extensive, and numerous other relevant references exist. For the sake of brevity, these will not be elaborated upon here; readers are encouraged to consult references [4], [9], [12], [15], [33], [36], [40], [43] for a more comprehensive exploration of the subject.

The Boussinesq equation stands as a pivotal tool in fluid dynamics and wave theory. It is employed to describe the propagation of long waves in shallow water, incorporating both nonlinear and dispersive effects. This equation facilitates the understanding of wave-water interactions and coastal processes, such as tsunamis and surf-zone waves. One of its commonly used forms is presented as follows:

$$u_{tt} + (u^2)_{xx} + u_{xxxx} = 0. \tag{2}$$

The term u_{tt} represents the second-order partial derivative of the function u with respect to time t. It reflects the temporal evolution characteristics of the wave. Physically, it stands for the acceleration of the system in the time dimension or the rate of change of the wave. The meanings of the two terms $(u^2)_{xx}$ and u_{xxxx} are similar to those in the KP equation. In summary, the Boussinesq equation incorporates temporal and spatial variations, along with nonlinear and dispersive effects, among other factors, and finds extensive applications in fields such as fluid mechanics and elasticity. In recent years, a wealth of cutting-edge research findings on the Boussinesq equation has emerged. For a more in-depth exploration, readers may refer to references [18], [21], [29], [34], [36], [41]. It is worth noting that beyond the works mentioned, a large body of related literature remains unlisted here.

In this paper, we integrate the characteristics of these two types of equations to investigate the following equation:

$$u_{tt} + u_{xt} + 6u_x^2 + 6uu_{xx} + u_{xxxx} - u_{yy} = 0. \tag{3}$$

Here, we refer to it as the Kadomtsev-Petviashvili-Boussinesq equation, abbreviated as the KPB equation. The Hirota bilinear method ([11], [13], [24]) stands as a pivotal approach for tackling nonlinear partial differential equations. Through ingenious transformations, it bilinearizes equations and constructs specific polynomials, thereby yielding exact solutions such as solitons and assisting researchers in unraveling the nonlinear world. By means of the dependent variable transformation $u = 2(\ln f)_{xx}$, we derive the Hirota bilinear form of Equation (3), which is detailed as follows.

$$\begin{aligned} &u_{tt} + u_{xt} + 6u_x^2 + 6uu_{xx} + u_{xxxx} - u_{yy} \\ &= \left[\frac{(D_t^2 + D_xD_t + D_x^4 - D_y^2)f \cdot f}{f^2}\right]_{xx} \\ &= 0, \end{aligned}$$

where D_x, D_y and D_t are Hirota's bilinear derivatives defined by

$$\begin{aligned} &D_x^{n_1} D_y^{n_2} D_t^{n_3} f \cdot g \\ &= \left(\frac{\partial}{\partial x} - \frac{\partial}{\partial x'}\right)^{n_1} \left(\frac{\partial}{\partial y} - \frac{\partial}{\partial y'}\right)^{n_2} \left(\frac{\partial}{\partial t} - \frac{\partial}{\partial t'}\right)^{n_3} \\ &f(x,y,t)g(x',y',t')|_{x=x',y=y',t=t'}. \end{aligned} \tag{4}$$

Therefore, the Hirota bilinear KPB equation is

$$\begin{aligned} &[D_t^2 + D_xD_t + D_x^4 - D_y^2]f \cdot f \\ =&2(f_{tt}f - f_t^2 + f_{xt}f - f_xf_t \\ &+ f_{xxxx}f - 4f_{xxx}f_x + 3f_{xx}^2 - f_{yy}f + f_y^2) \\ =&0. \end{aligned} \tag{5}$$

The bilinear equation (5) forms the foundation for subsequent investigations into various solutions of the KPB equation. The structure of this paper is as follows:

In Section II, we examine the two-soliton solutions of the KPB equation, and select a set of parameters to present three dimensional and contour plots of these soliton solutions.

In Section III, we derive the breather solutions of the KPB equation and plot their corresponding graphs. These figures reveal that the breather solutions exhibit distinct periodicity.

In Sections IV and V, we analyze the lump solutions and interaction solutions of the KPB equation, respectively, and provide their three dimensional and contour plots.

In Section VI, we incorporate the dynamical behaviors of the double pendulum system into the variables of the aforementioned soliton, breather, lump, and interaction solutions, aiming to investigate the chaotic behaviors exhibited by these solutions.

Finally, in Section VII, we present our conclusions.

II. Soliton solutions

The soliton solutions of PDEs have long been a focus of significant research interest (see [6], [7], [8], [16], [20], [21], [23], [25], [28], [33], [35], [36], [37], [38], [42], [44]). Solitons are stable, localized wave packets that retain their shape during propagation. Within the two dimensional framework of the KPB equation, these soliton solutions exhibit distinctive characteristics: they describe wave phenomena involving interactions in a planar space, as opposed to one-dimensional linear propagation. Such solutions facilitate the understanding of various physical processes, including the behavior of waves in specific nonlinear media. Their investigation yields insights into complex wave dynamics and is thus crucial for applications in fields such as fluid dynamics and plasma physics.

In this part, only the two-dimensional soliton solutions will be discussed. It is assumed that the soliton solutions of the KPB equation can be expressed as

$$f = 1 + a_7e^g + a_8e^h + a_9e^{g+h}, \tag{6}$$

where $g = a_1x + a_2y + a_3t, h = a_4x + a_5y + a_6t$. Substituting (6) into (5), the following system of equations

can be obtained.

$$\begin{cases} a_8a_9(a_1^4+a_1a_3-a_2^2+a_3^2)=0; \\ a_7a_9(a_4^4+a_4a_6-a_5^2+a_6^2)=0; \\ (a_1^4-4a_1^3a_4+6a_1^2a_4^2+(-4a_4^3+a_3-a_6)a_1+a_4^4 \\ +(-a_3+a_6)a_4-(a_2+a_3-a_5-a_6)(a_2-a_3 \\ -a_5+a_6))a_8a_7+a_9(a_1^4+4a_1^3a_4+6a_1^2a_4^2 \\ +(4a_4^3+a_3+a_6)a_1+a_4^4+(a_3+a_6)a_4 \\ -(a_2+a_3+a_5+a_6)(a_2-a_3+a_5-a_6))=0; \\ a_7(a_1^4+a_1a_3-a_2^2+a_3^2)=0; \\ a_8(a_4^4+a_4a_6-a_5^2+a_6^2)=0. \end{cases} \tag{7}$$

This system of equations can be solved using Maple software, yielding multiple sets of solutions that will not be elaborated on in detail here. Instead, a single set of solutions is selected for numerical simulation to generate its corresponding images. Set $a_1=0, a_2=1, a_3=1, a_4=-1/2, a_5=-9/4, a_6=-2, a_7=a_8=a_9=1$, we obtain one of the soliton solution as

$$\begin{aligned} &u(x,y,t)_{\text{Soliton}} \\ =&\frac{2\left(\frac{\mathrm{e}^{-\frac{x}{2}-\frac{9y}{4}-2t}}{4}+\frac{\mathrm{e}^{-\frac{5y}{4}-t-\frac{x}{2}}}{4}\right)}{\left(1+\mathrm{e}^{y+t}+\mathrm{e}^{-\frac{x}{2}-\frac{9y}{4}-2t}+\mathrm{e}^{-\frac{5y}{4}-t-\frac{x}{2}}\right)^2} \\ &\times\frac{\left(1+\mathrm{e}^{y+t}+\mathrm{e}^{-\frac{x}{2}-\frac{9y}{4}-2t}+\mathrm{e}^{-\frac{5y}{4}-t-\frac{x}{2}}\right)}{\left(1+\mathrm{e}^{y+t}+\mathrm{e}^{-\frac{x}{2}-\frac{9y}{4}-2t}+\mathrm{e}^{-\frac{5y}{4}-t-\frac{x}{2}}\right)^2} \\ &-\frac{2\left(-\frac{\mathrm{e}^{-\frac{x}{2}-\frac{9y}{4}-2t}}{2}-\frac{\mathrm{e}^{-\frac{5y}{4}-t-\frac{x}{2}}}{2}\right)^2}{\left(1+\mathrm{e}^{y+t}+\mathrm{e}^{-\frac{x}{2}-\frac{9y}{4}-2t}+\mathrm{e}^{-\frac{5y}{4}-t-\frac{x}{2}}\right)^2}. \end{aligned} \tag{8}$$

We present this two-dimensional soliton solution images when $x=0$ and $x=10$, as shown in Figure 1, 2, 3 and 4.

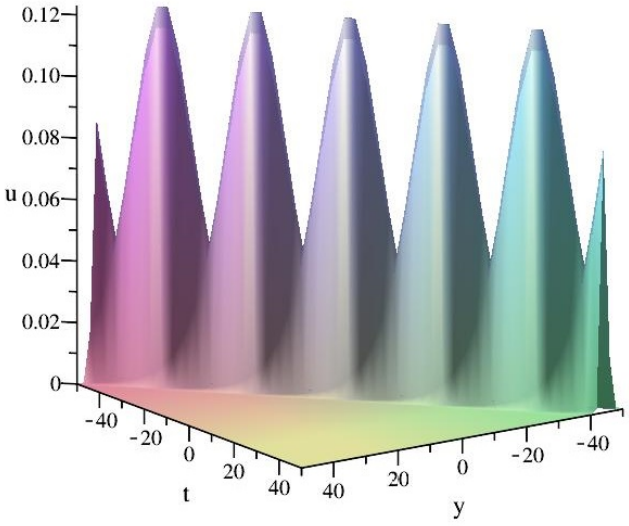

Fig. 1. 3D plot of $u(x,y,t)_{\text{Soliton}}$ for $x=0$.

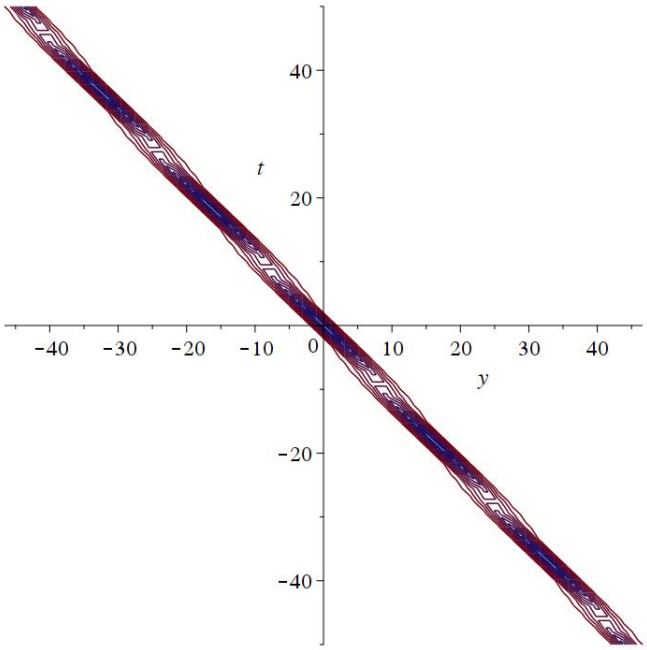

Fig. 2. Contour plot of $u(x,y,t)_{\text{Soliton}}$ for $x=0$.

III. Breather solutions

The breather solution ([3], [5]) in nonlinear partial differential equations describes localized, periodically varying phenomena in physical systems. In the context of water waves, it manifests as the periodic aggregation and dispersion of energy within a localized region, analogous to oceanic wave packets. Studying such solutions facilitates understanding of their formation, propagation, and interactions—knowledge that is critical for marine engineering structures. In shallow water models, it captures variations in surface undulations. Additionally, it characterizes the behavior of light pulses in nonlinear optical materials, which proves valuable in fiber-optic communications for analyzing signal distortion and recovery. Unlike soliton solutions, which maintain a constant shape during propagation, breather solutions undergo periodic changes. While traveling wave solutions propagate at a constant speed in a specific direction, breather solutions are distinguished by their focus on localized periodic variations.

In the follows, let's study the breather solution of the KPB equation (3). Suppose its breather solution has the following expression form:

$$f=e^{-g}+a_7\sin(h)+a_8e^{g}, \tag{9}$$

where

$$g=a_1x+a_2y+a_3t,$$

$$h=a_4x+a_5y+a_6t,$$

$a_i(i=1,2\cdots,8)$ are constants to be determined.

Using Maple software, substitute (9) into the equation (5). Combine like terms of the product of trigonometric functions and exponential functions, and then set their coefficients to be zero. We can obtain the following system of equations.

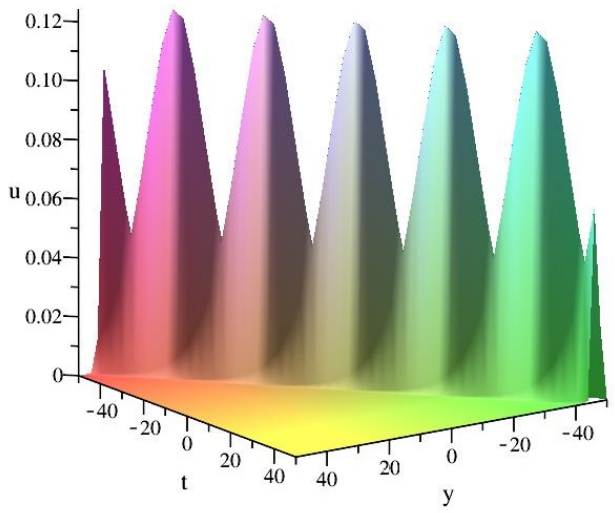

Fig. 3. 3D plot of $u(x,y,t)_{\text{Soliton}}$ for $x=10$.

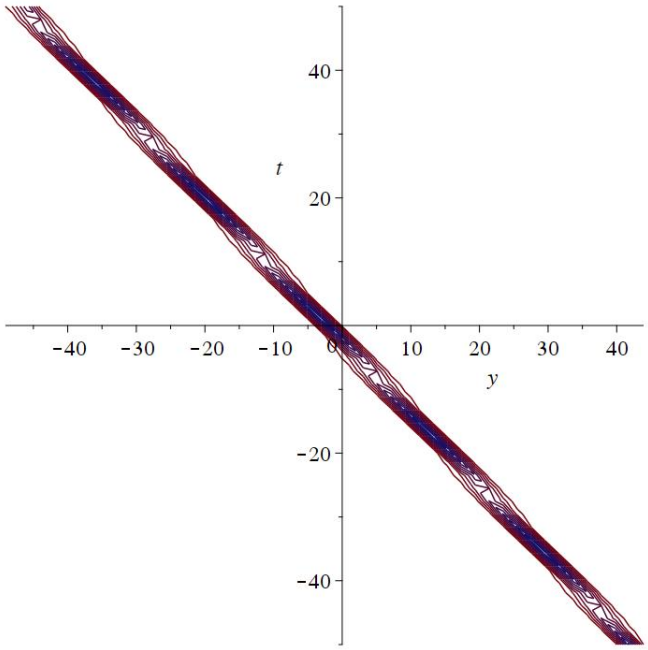

Fig. 4. Contour plot of $u(x,y,t)_{\text{Soliton}}$ for $x=10$.

$$\begin{cases} a_1^4-6a_1^2a_4^2+a_4^4+a_3a_1-a_2^2+a_3^2 \\ -a_4a_6+a_5^2-a_6^2=0; \\ 4a_1^3a_4-4a_1a_4^3+a_1a_6-2a_2a_5+ \\ a_3a_4+2a_3a_6=0; \\ 4a_4^4-a_4a_6+a_5^2-a_6^2=0; \\ 4a_1^4+a_3a_1-a_2^2+a_3^2=0. \end{cases} \tag{10}$$

By solving this algebraic system of equations (10) through Maple software, many cases of solutions can be obtained as follows.

Case 1: $a_1=-1/4, a_2=-a_3+1/8, a_3=a_3, a_4=\pm i/4, a_5=-a_6\mp i/8, a_6=a_6, a_7=a_7, a_8=a_8$;

Case 2: $a_1=-1/4, a_2=a_3-1/8, a_3=a_3, a_4=\pm i/4, a_5=a_6+\pm i/8, a_6=a_6, a_7=a_7, a_8=a_8$;

Case 3: $a_1=1/4, a_2=-a_3-1/8, a_3=a_3, a_4=\pm i/4, a_5=-a_6\mp i/8, a_6=a_6, a_7=a_7, a_8=a_8$;

Case 4: $a_1=1/4, a_2=a_3+1/8, a_3=a_3, a_4=\pm i/4, a_5=a_6+\pm i/8, a_6=a_6, a_7=a_7, a_8=a_8$;

Case 5: $a_1=Z_1, a_2=a_2, a_3=a_3, a_4=Z_2, a_5=\frac{1}{2a_2}(8Z_1^3Z_2+2a_3^2Z_3+a_3Z_1Z_3+a_3Z_2), a_6=a_3Z_3, a_7=a_7, a_8=a_8$, where Z_1 satisfies equation

$$4Z_1^4+Z_1a_3-a_2^2+a_3^2=0;$$

Z_2 satisfies equation

$$Z_2^2+Z_1^2=0,$$

Z_3 satisfies equation

$$(a_2^2-a_3^2)Z_3^2-(8Z_1^3Z_2+2a_3Z_2)Z_3-a_2^2+a_3^2=0.$$

Substituting (9) into $u=2(\ln f)_{xx}$ it can obtain the breather solution of the KPB equation (3) as follows.

$$\begin{aligned} u(x,y,t)=&\frac{2(a_8a_1^2e^g+a_1^2e^{-g}-a_7a_4^2\sin h)}{e^{-g}+a_7\sin h+a_8e^g} \\ &-\frac{2(a_8a_1e^g-a_1e^{-g}+a_7a_4\cos h)^2}{(e^{-g}+a_7\sin h+a_8e^g)^2}. \end{aligned} \tag{11}$$

In order to better intuitively observe the graphics and dynamic properties of the breather solution, we select a group of parameters to draw its three-dimensional plot, contour plot and density plot. Set $a_1=-1/4,\ a_2=-7/8,\ a_3=1,\ a_4=i/4,\ a_5=-1-i/8,\ a_6=1,\ a_7=1,\ a_8=1$. Substituting this group of values into equation (11), we get the solution $u(x,y,t)_{\text{Breather}}$ and use Maple software to draw a 3D image with x,y and $Re(u)$ as coordinate axes. Three cases of $t=-2,0,2$ are selected respectively. At the same time, their corresponding contour plots and density plots are also drawn. See Figures 5, 6, 7, 8, 9, 10, 11, 12 and 13 for details.

IV. Lump solutions

The lump solution of partial differential equations ([6], [9], [10], [19], [26], [31], [33], [35], [39], [40]) is a distinctive localized solution. It manifests as an isolated, lump-like structure in space, typically taking the form of a rational function with energy concentrated within a limited region and values decaying rapidly away from the center. In fluid mechanics, it can simulate localized vortices; in nonlinear optics, it facilitates the understanding of the formation and interaction of optical solitons, which hold potential for information transmission. The study of lump solutions enables a deeper comprehension of localized behaviors and energy aggregation in complex systems described by partial differential equations, thereby offering a new perspective for exploring the internal mechanisms of complex physical systems.

We assume that the lump solution of the KPB equation (3) has the following form.

$$f=g^2+h^2+a_7, \tag{12}$$

where

$$g=a_1x+a_2y+a_3t,$$
$$h=a_4x+a_5y+a_6t,$$

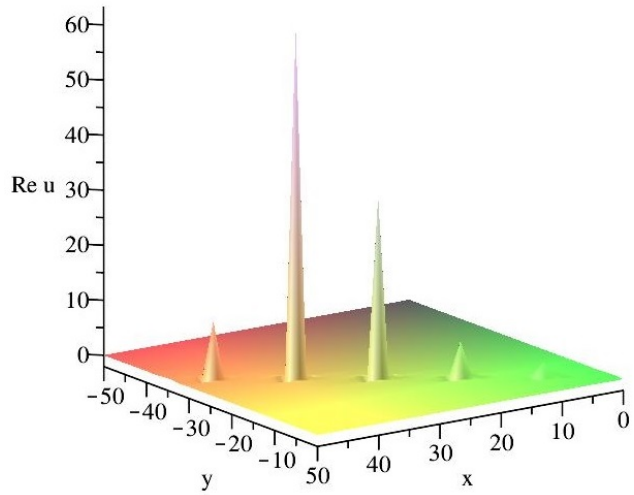

Fig. 5. 3D plot of $u(x, y, t)_{\text{Breather}}$ for $t = -2$.

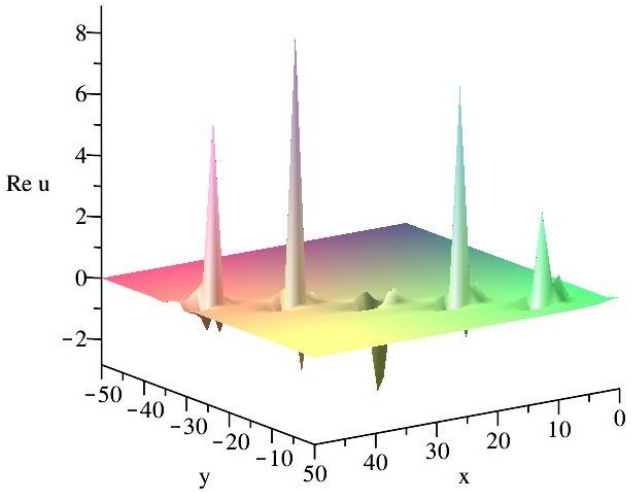

Fig. 8. 3D plot of $u(x, y, t)_{\text{Breather}}$ for $t = 0$.

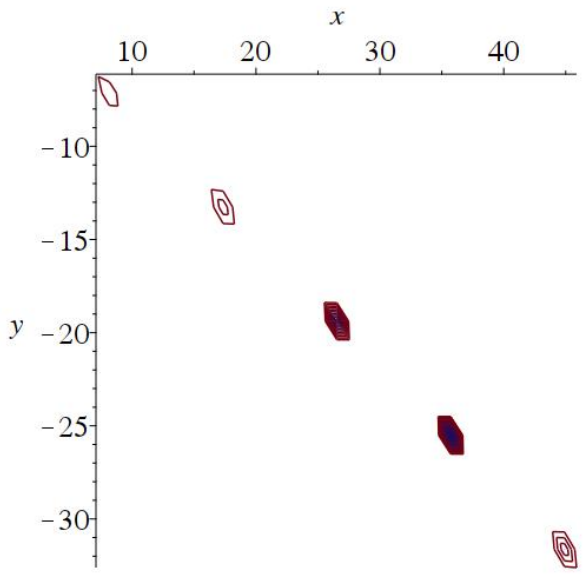

Fig. 6. Contour plot of $u(x, y, t)_{\text{Breather}}$ for $t = -2$.

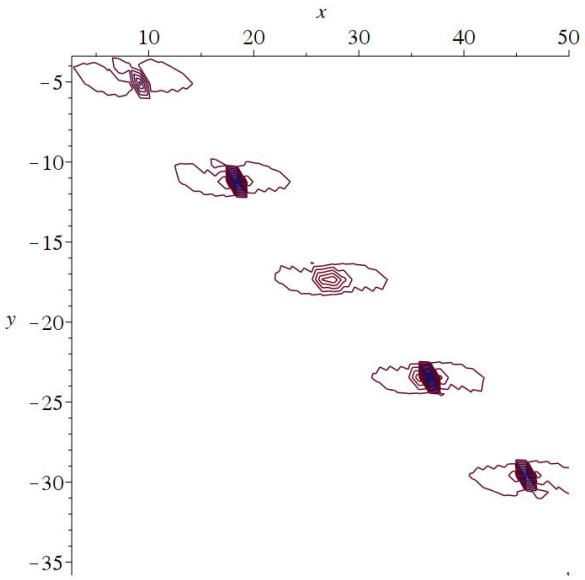

Fig. 9. Contour plot of $u(x, y, t)_{\text{Breather}}$ for $t = 0$.

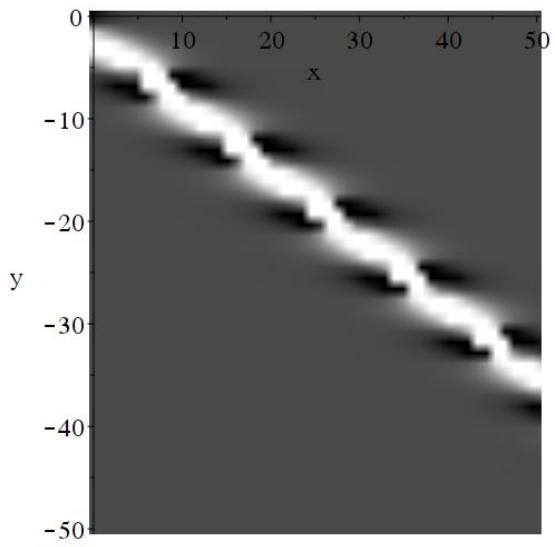

Fig. 7. Density plot of $u(x, y, t)_{\text{Breather}}$ for $t = -2$.

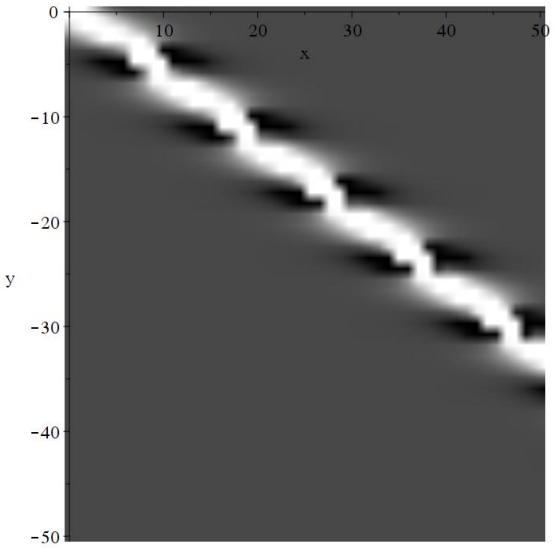

Fig. 10. Density plots of $u(x, y, t)_{\text{Breather}}$ for $t = 0$.

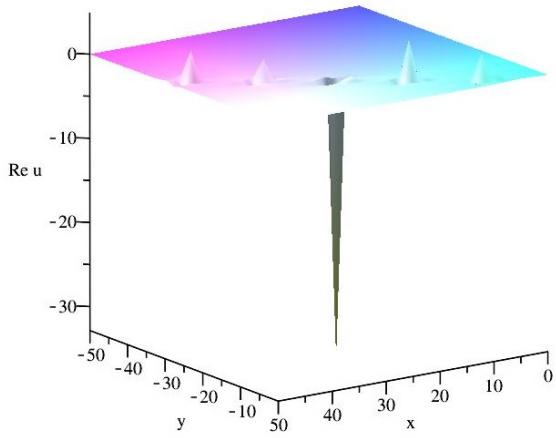

Fig. 11. 3D plot of $u(x,y,t)_{\text{Breather}}$ for $t=2$.

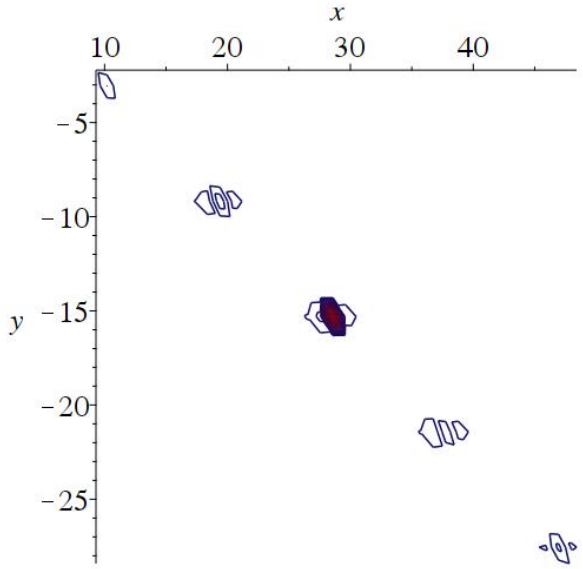

Fig. 12. Contour plot of $u(x,y,t)_{\text{Breather}}$ for $t=2$.

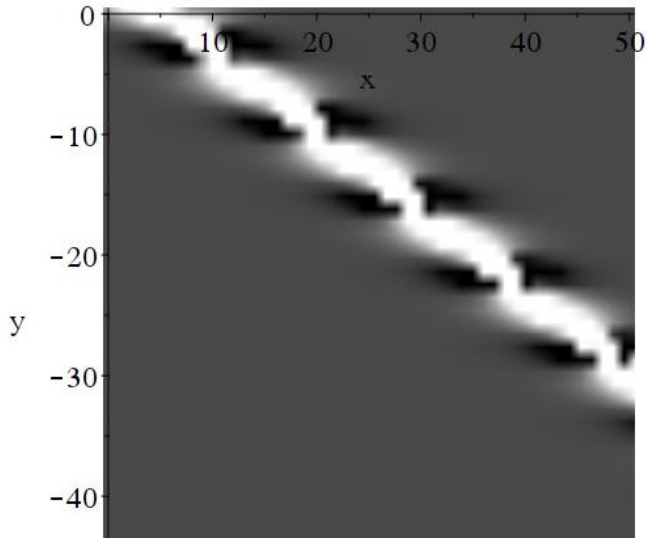

Fig. 13. Density plots of $u(x,y,t)_{\text{Breather}}$ for $t=2$.

$a_i (i=1,2\cdots,7)$ are constants to be determined.

We substitute (12) into equation (5), and combine the terms related to x, y and t, then obtain seven equations. Solving this system of equations by Maple software gives the following solutions.

Case 1

$a_1 = -\frac{a_4(\pm i+1)}{\pm i-1},\ a_2 = \pm i a_5,\ a_3 = 0,\ a_4 = a_4,\ a_5 = a_5,\ a_6 = a_6,\ a_7 = a_7.$

Case 2

$a_1 = a_1,\ a_2 = \pm i a_5,\ a_3 = \pm i a_6,\ a_4 = a_4,\ a_5 = Z_1,\ a_6 = a_6,\ a_7 = -\frac{6(a_1^2+a_2^2)^2}{a_6(\pm i a_1+a_4)}$, where Z_1 satisfies $2Z_1^2 \pm i a_1 a_6 - a_4 a_6 - 2a_6^2 = 0$.

Case 3

$a_1 = \pm i a_4,\ a_2 = \pm i a_5,\ a_3 = \pm i a_6,\ a_4 = a_4,\ a_5 = a_5,\ a_6 = a_6,\ a_7 = a_7.$

Case 4

$$
\begin{aligned}
a_1 =&(a_2^2a_3 + 2a_5a_6a_2 - a_3^3 - a_5^2a_3 - a_6^2a_3)/(a_3^2 + a_6^2),\\
a_2 =&a_2, a_3 = a_3,\\
a_4 =&-(a_6a_2^2 - 2a_5a_2a_3 + a_6a_3^2 - a_5^2a_6 + a_6^3)/(a_3^2 + a_6^2),\\
a_5 =&a_5,\ a_6 = a_6,\\
a_7 =&3(a_2^8 - 4a_2^6a_3^2 + 4a_2^6a_5^2 + 4a_2^6a_6^2 - 16a_2^5a_3a_5a_6\\
&+ 6a_2^4a_3^4 - 4a_2^4a_3^2a_5^2 - 4a_2^4a_3^2a_6^2 + 6a_2^4a_5^4 + 4a_2^4a_5^2a_6^2\\
&+ 6a_2^4a_6^4 + 32a_2^3a_3^3a_5a_6 - 32a_2^3a_3a_5^3a_6 - 32a_2^3a_3a_5a_6^3\\
&- 4a_2^2a_3^6 - 4a_2^2a_3^4a_5^2 - 4a_2^2a_3^4a_6^2 + 4a_2^2a_3^2a_5^4\\
&+ 88a_2^2a_3^2a_5^2a_6^2 + 4a_2^2a_3^2a_6^4 + 4a_2^2a_5^6 - 4a_2^2a_5^4a_6^2\\
&- 4a_2^2a_5^2a_6^4 + 4a_2^2a_6^6 - 16a_2a_3^5a_5a_6 - 32a_2a_3^3a_5^3a_6\\
&- 32a_2a_3^3a_5a_6^3 - 16a_2a_3a_5^5a_6 + 32a_2a_3a_5^3a_6^3\\
&- 16a_2a_3a_5a_6^5 + a_3^8 + 4a_3^6a_5^2 + 4a_3^6a_6^2 + 6a_3^4a_5^4\\
&+ 4a_3^4a_5^2a_6^2 + 6a_3^4a_6^4 + 4a_3^2a_5^6 - 4a_3^2a_5^4a_6^2\\
&- 4a_3^2a_5^2a_6^4 + 4a_3^2a_6^6 + a_5^8 - 4a_5^6a_6^2 + 6a_5^4a_6^4\\
&- 4a_5^2a_6^6 + a_6^8)/((a_2a_6 - a_3a_5)^2(a_3^2 + a_6^2)).
\end{aligned}
$$

In order to describe the lump solution intuitively, we set the values of the parameters according to the above solutions. Set $a_1 = -8/5, a_2 = 1, a_3 = 2, a_4 = -9/5, a_5 = 3, a_6 = 4, a_7 = 2523/5$, then we have that

$$
\begin{aligned}
&u(x,y,t)_{\text{Lump}} =\\
&\frac{2\left(\frac{58\left(-\frac{8x}{5}+y+2t\right)^2}{5} + \frac{58\left(-\frac{9x}{5}+3y+4t\right)^2}{5}\right)}{\left(\left(-\frac{8x}{5}+y+2t\right)^2 + \left(-\frac{9x}{5}+3y+4t\right)^2 + \frac{2523}{5}\right)^2}\\
&+\frac{2\left(\frac{146334}{25} - \left(\frac{58x}{5} - 14y - \frac{104t}{5}\right)^2\right)}{\left(\left(-\frac{8x}{5}+y+2t\right)^2 + \left(-\frac{9x}{5}+3y+4t\right)^2 + \frac{2523}{5}\right)^2}.
\end{aligned}
\tag{13}
$$

Set $t = -2, 0, 2$ respectively to obtain the images of $u(x,y,t)_{\text{Lump}}$. The corresponding images can be found in Figures 20, 21, 22, 14, 15, 16, 17, 18 and 19.

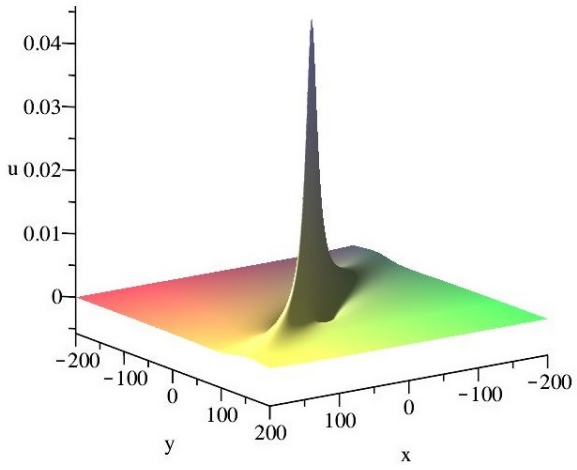

Fig. 14. 3D plot of $u(x, y, t)_{\text{Lump}}$ for $t = 0$.

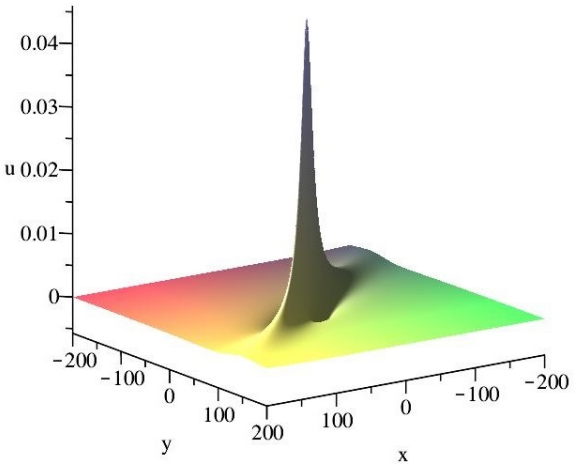

Fig. 17. 3D plot of $u(x, y, t)_{\text{Lump}}$ for $t = 2$.

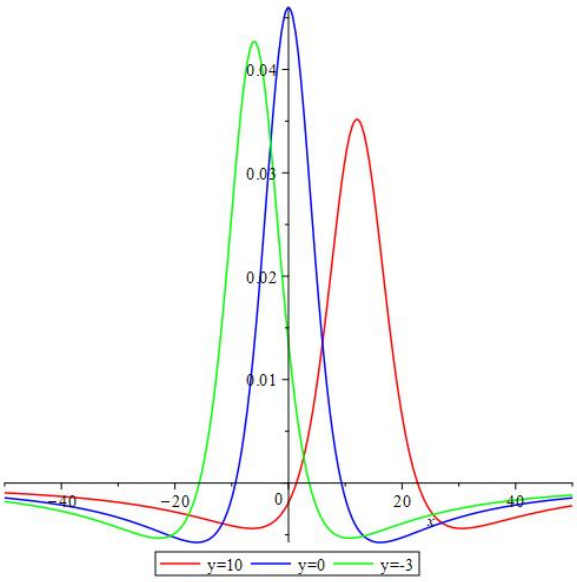

Fig. 15. 2D plot of $u(x, y, t)_{\text{Lump}}$ for $t = 0$.

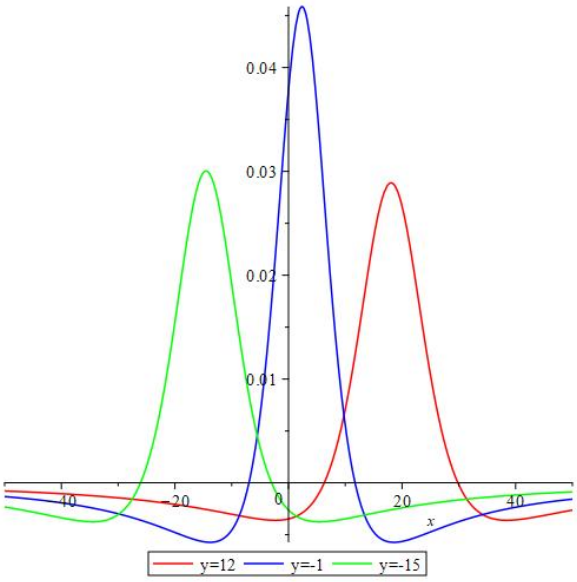

Fig. 18. 2D plot of $u(x, y, t)_{\text{Lump}}$ for $t = 2$.

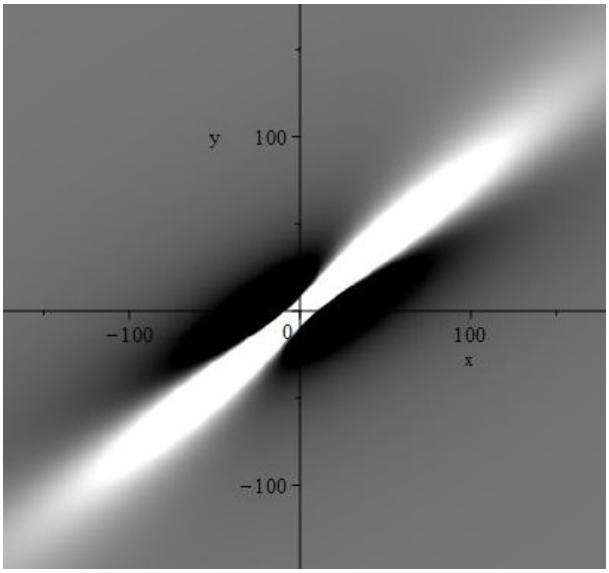

Fig. 16. Density plot of $u(x, y, t)_{\text{Lump}}$ for $t = 0$.

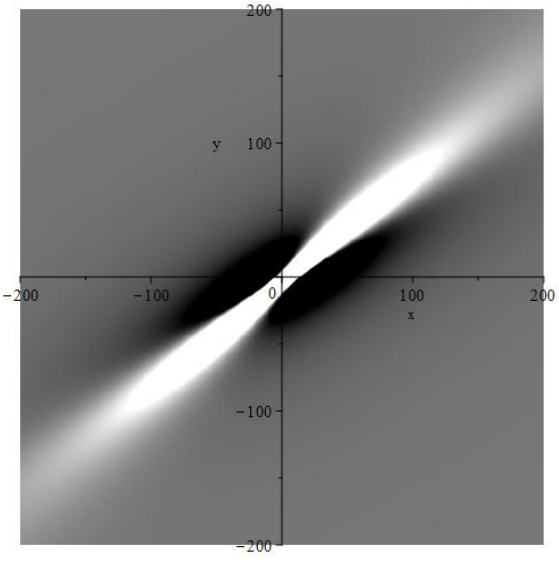

Fig. 19. Density plot of $u(x, y, t)_{\text{Lump}}$ for $t = 2$.

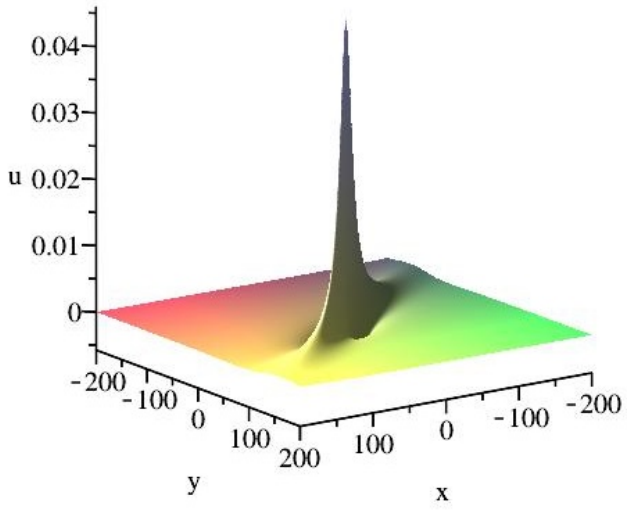

Fig. 20. 3D plot of $u(x, y, t)_{\text{Lump}}$ for $t = -2$.

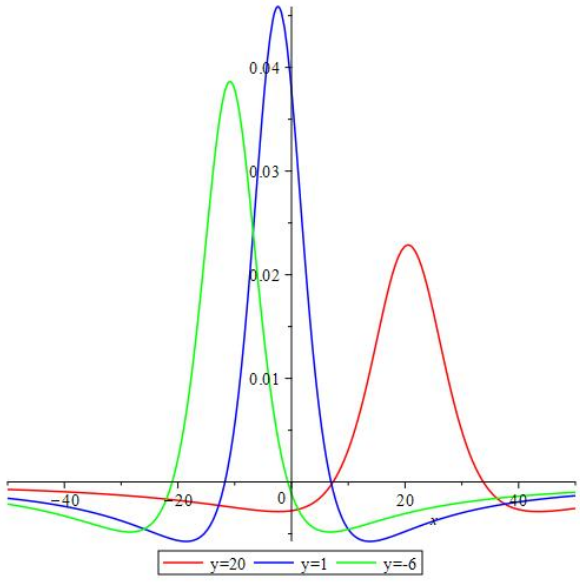

Fig. 21. 2D plot of $u(x, y, t)_{\text{Lump}}$ for $t = -2$.

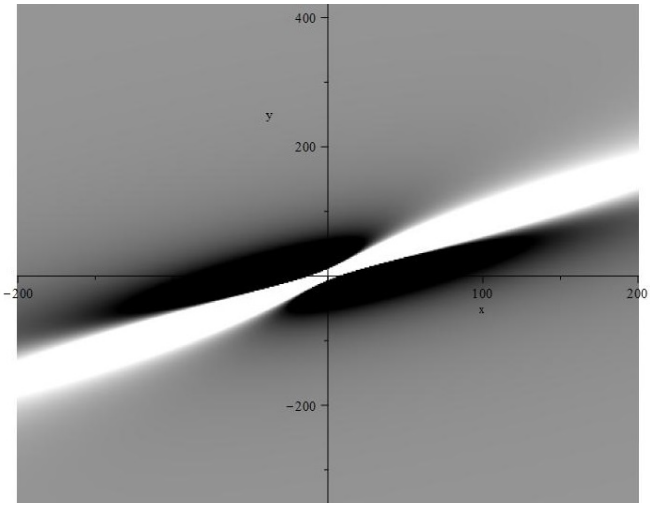

Fig. 22. Density plot of $u(x, y, t)_{\text{Lump}}$ for $t = -2$.

V. Interaction between Lump solutions and hyperbolic cosine functions

The interaction between lump solutions and hyperbolic cosine functions holds significant importance [22]. A lump solution is a distinct localized solution in partial differential equations, characterized by spatial isolation, with energy or amplitude concentrated within a limited region and decaying rapidly outside this domain. The hyperbolic cosine function possesses unique morphological features and properties. Their interaction implies inherent connections in both the mathematical structure and physical implications of partial differential equations. In physical systems, such interactions are of critical relevance. In fluid mechanics, they can model interactions between different wave types, thereby facilitating the understanding of complex fluid flow behaviors. In nonlinear optics, they help explain the interaction mechanisms between light pulses and background fields, which is beneficial for optical device design and communication system optimization. Mathematically, this interaction enriches the theory of solutions to partial differential equations. In engineering applications, it provides potential avenues for optimizing designs—such as shock absorbers and electromagnetic shields—by enabling more precise control and utilization of energy distribution. Thus, it carries extensive implications and value across multiple fields.

For the KPB equation in this paper, it is assumed that its interaction solution has the following form:

$$f = g^2 + h^2 + l, \tag{14}$$

where

$$g = a_1 x + a_2 y + a_3 t,$$

$$h = a_4 x + a_5 y + a_6 t,$$

$$l = \cosh(a_7 x + a_8 y + a_9 t),$$

and $a_i (i = 1, 2 \cdots, 9)$ are constants to be determined.

Substitute (14) into the bilinear equation (5). By combining like terms and setting the corresponding coefficients to zero, a system of 17 equations can be obtained. Solve it using the Maple software, and the following four groups of solutions are obtained.

Case 1

$a_1 = \pm i a_4, a_2 = \pm i a_5, a_3 = 0, a_4 = a_4, a_5 = a_5, a_6 = 0, a_7 = a_7, a_8 = -4a_7^3, a_9 = -4a_7^3$;

Case 2

$a_1 = -\frac{a_4(\pm i+1)}{\pm i-1}, a_2 = \pm i a_5, a_3 = 0, a_4 = a_4, a_5 = a_5, a_6 = 0, a_7 = 0, a_8 = 0, a_9 = 0$;

Case 3

$a_1 = \pm i a_4, a_2 = \pm i a_5, a_3 = 0, a_4 = a_4, a_5 = a_5, a_6 = 0, a_7 = a_7, a_8 = 4a_7^3, a_9 = -4a_7^3$.

Case 4

$a_1 = \pm i a_4,\ a_2 = \pm i a_5,\ a_3 = \pm i a_6,\ a_4 = a_4,\ a_5 = a_5,\ a_6 = a_6,\ a_7 = a_7,\ a_8 = \sqrt{4a_7^4 + a_7 a_9 + a_9^2},\ a_9 = a_9$.

Therefore, we set $a_1 = 2i, a_2 = i, a_3 = 0, a_4 = 2, a_5 = 1, a_6 = 0, a_7 = 1, a_8 = -4, a_9 = -4$, and obtained a specific interaction solution of the KPB equation.

$$
\begin{aligned}
&u(x,y,t)_{\text{Interaction}} = \\
&\frac{2\cosh(-x+4y+4t)}{((2ix+iy)^2+(2x+y)^2+\cosh(-x+4y+4t))^2} \\
&\times \frac{((2ix+iy)^2+(2x+y)^2+\cosh(-x+4y+4t))}{((2ix+iy)^2+(2x+y)^2+\cosh(-x+4y+4t))^2} \\
&- \frac{2(4i(2ix+iy)+8x+4y-\sinh(-x+4y+4t))^2}{((2ix+iy)^2+(2x+y)^2+\cosh(-x+4y+4t))^2}.
\end{aligned} \tag{15}
$$

Then its graph is presented, with details shown in Figures 23, 24, 25 26, 27, 28, 29, 30 and 31.

VI. Chaotic behavior

A double pendulum ([1], [17], [27], [30], [45]) is a physical system composed of two pendulums attached end-to-end. The first pendulum is attached to a fixed point, and the second pendulum is attached to the end of the first one. Mathematically, let the length and the mass of the first pendulum be L_1 and m_1, the length and the mass of the second pendulum be L_2 and m_2. The angles that the first and second pendulums make with the vertical direction are usually denoted as θ and ϕ respectively, see Figure 32.

The motion of a double pendulum system is described by a set of nonlinear differential equations. Using Lagrangian mechanics, the Lagrangian L of the system is given by the difference between the kinetic energy T and the potential energy V of the system. The kinetic energy of the double pendulum is

$$
\begin{aligned}
T :=& \frac{1}{2} m_1 L_1^2 \dot{\theta}^2 + \\
& \frac{1}{2} m_2 \left[L_1^2 \dot{\theta}^2 + L_2^2 \dot{\phi}^2 + 2 L_1 L_2 \dot{\theta} \dot{\phi} \cos(\theta - \phi) \right],
\end{aligned} \tag{16}
$$

where $\dot{\theta}$ and $\dot{\phi}$ denote the derivative of θ and ϕ with respect to time s respectively. The potential energy is

$$V := m_1 g L_1 \cos\theta + m_2 g \left(L_1 \cos\theta + L_2 \cos\phi \right).$$

The dynamics of the double pendulum can be studied via the Euler-Lagrange equations

$$
\begin{cases}
\frac{d}{ds}\left(\frac{\partial L}{\partial \dot{\theta}}\right) - \frac{\partial L}{\partial \theta} = 0; \\
\frac{d}{ds}\left(\frac{\partial L}{\partial \dot{\phi}}\right) - \frac{\partial L}{\partial \phi} = 0,
\end{cases} \tag{17}
$$

where Lagrange function $L := T - V$. One of the most interesting aspects of the double pendulum system is its chaotic behavior. Even for a small number of degrees of freedom (two in this case), the system can exhibit extremely complex and unpredictable motion. The sensitivity of the system to initial conditions is a characteristic of chaos. A very small change in the initial angles θ and ϕ or the initial angular velocities $\dot{\theta}(0)$ and $\dot{\phi}(0)$ can lead to a completely different long-term behavior of the pendulums. For convenience, let's assume that the two pendulums are the same, that is, $L_1 = L_2 = 1$ and $m_1 = m_2 = m$. We pick initial conditions as one pendulum on top of the other

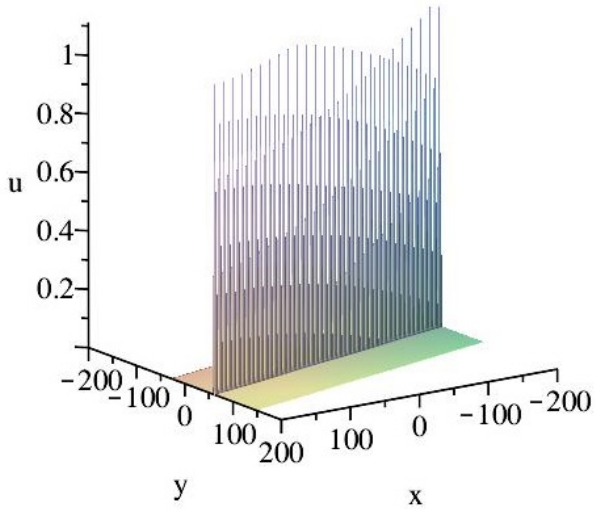

Fig. 23. 3D plot of the interaction solution for $t = -10$.

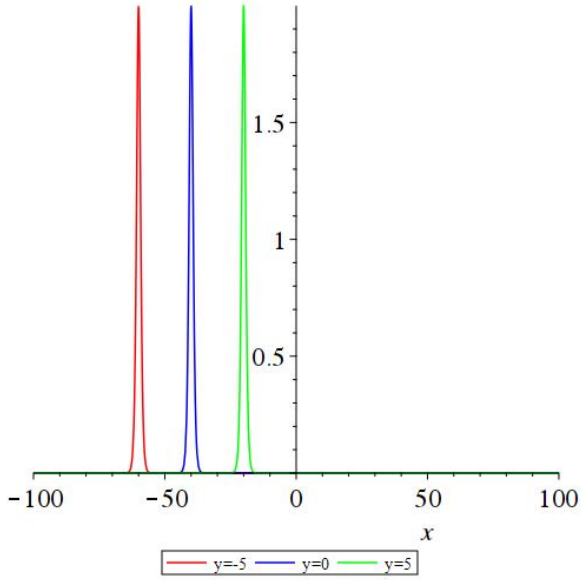

Fig. 24. 2D plot of the interaction solution for $t = -10$.

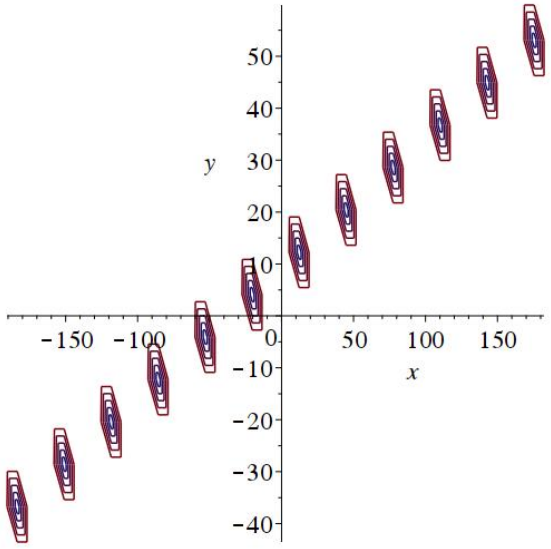

Fig. 25. Contour plot of the interaction solution for $t = -10$.

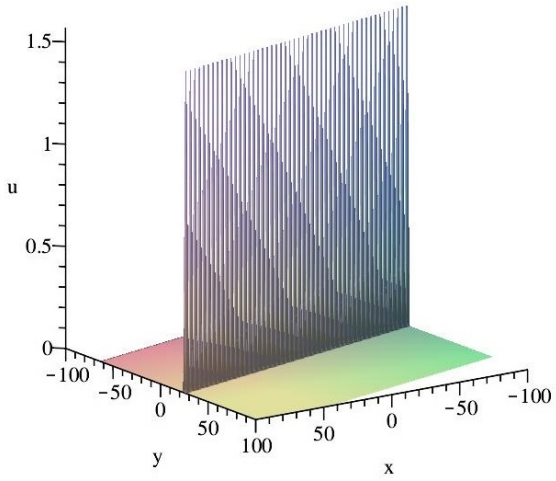

Fig. 26. 3D plot of the interaction solution for $t = 0$.

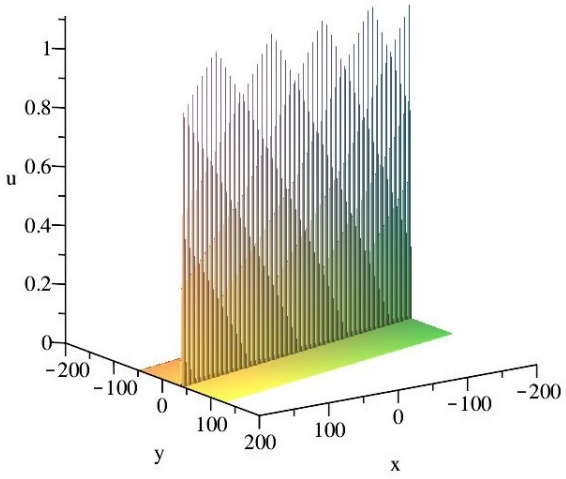

Fig. 29. 3D plot of the interaction solution for $t = 10$.

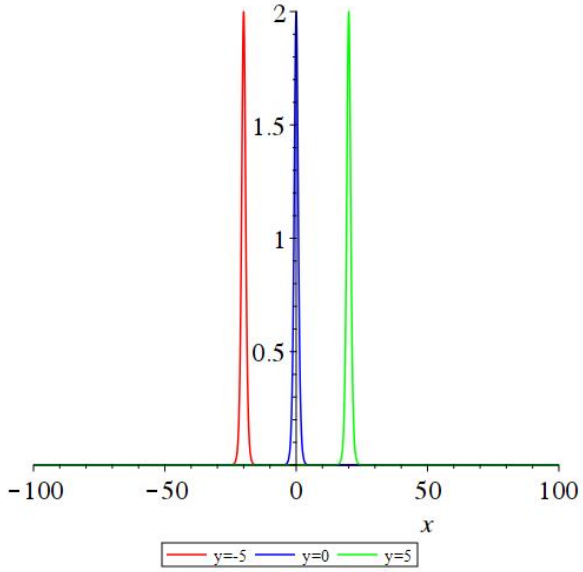

Fig. 27. 2D plot of the interaction solution for $t = 0$.

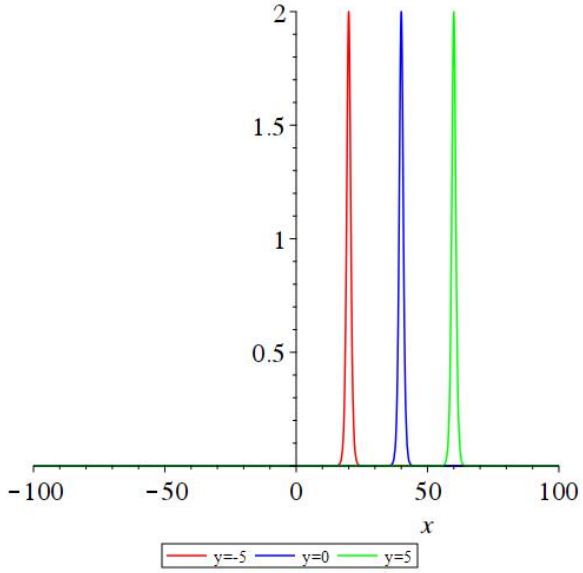

Fig. 30. 2D plot of the interaction solution for $t = 10$.

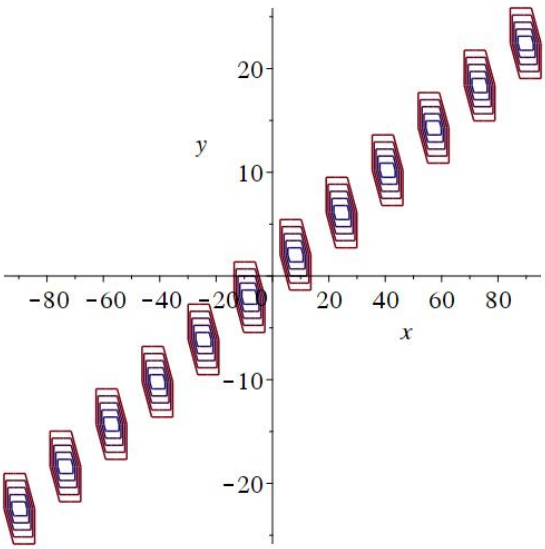

Fig. 28. Contour plot of the interaction solution for $t = 0$.

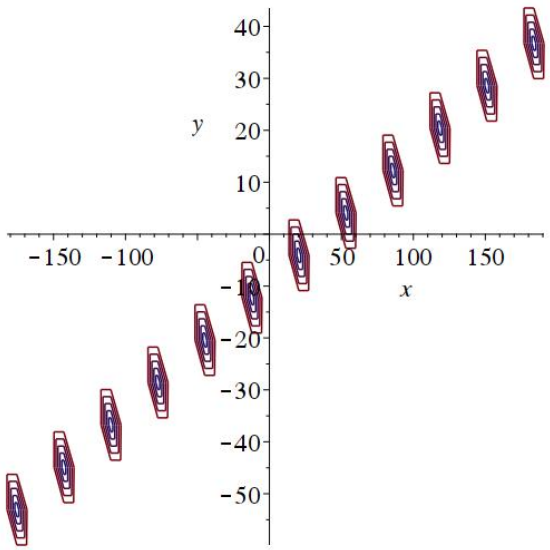

Fig. 31. Contour plot of the interaction solution for $t = 10$.

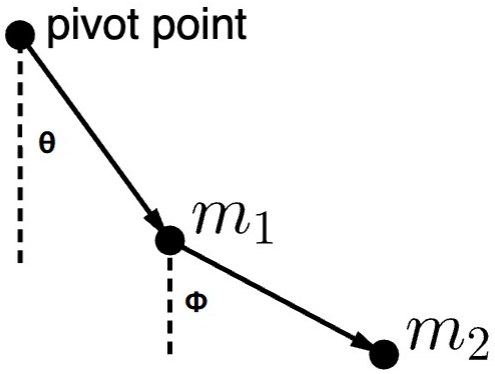

Fig. 32. The double pendulum system.

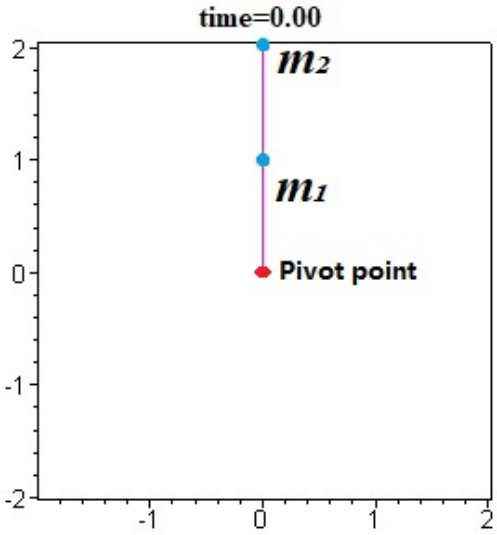

Fig. 33. The initial positions of the double pendulum system.

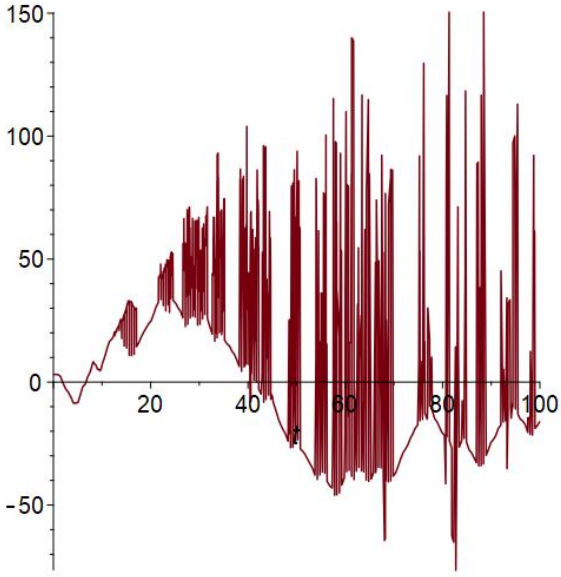

Fig. 34. Chaotic behavior of $\theta(s)$.

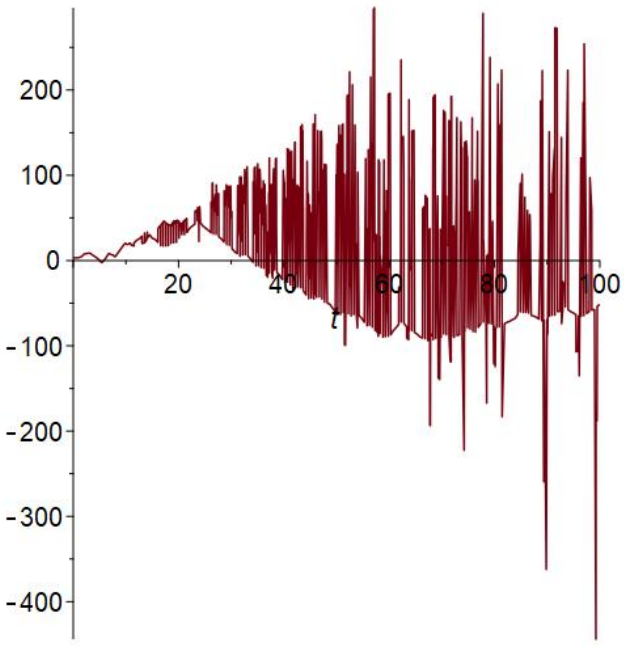

Fig. 35. Chaotic behavior of $\phi(s)$.

(unstable equilibrium) and the initial conditions of the Euler-Lagrange equations (17) are

$$\theta(0) = \pi,\ \dot{\theta}(0) = -0.01,\ \phi(0) = \pi,\ \dot{\phi}(0) = 0.$$

For a more intuitive understanding, one can refer to Figure 33. The chaotic behaviors of $\theta(s)$ and $\phi(s)$ with respect to time s can be seen in Figure 34 and 35.

The primary feature of this paper lies in applying the chaotic behaviors of $\theta(s)$ and $\phi(s)$ from the double pendulum system to various solutions of the KPB equation. The chaotic behavior in the double pendulum system is relatively intuitive, characterized by high sensitivity to initial conditions and the unpredictability of long-term dynamics. By incorporating such chaotic behavior into the solutions of the KPB equation, we can investigate the properties of these solutions from a novel perspective. It is plausible to observe that, within specific parameter ranges, the solutions of the KPB equation also exhibit chaos-like complex structures—findings that contribute to a deeper understanding of chaotic phenomena across different mathematical physics models.

When the chaotic behavior of the double pendulum system is introduced into a variable of the KPB equation's solutions, originally regular solutions (e.g., soliton solutions, breather solutions, lump solutions) may undergo irregular changes in both temporal and spatial domains. These changes no longer follow simple periodic or predictable patterns but instead embody the uncertainty and complexity inherent to chaotic systems. This makes the description of solution behaviors more aligned with real-world complex scenarios, such as turbulent flows in water waves or wave motions in water areas subjected to complex external disturbances.

Firstly, we substitute $\theta(s)$ and $\phi(s)$ for the variable y in the soliton solution (8). We then use Maple software to generate their corresponding graphs, as shown in Figures 36, 37, 38 and 39. By comparing the contour plots before and after the introduction of chaotic behavior (specifically,

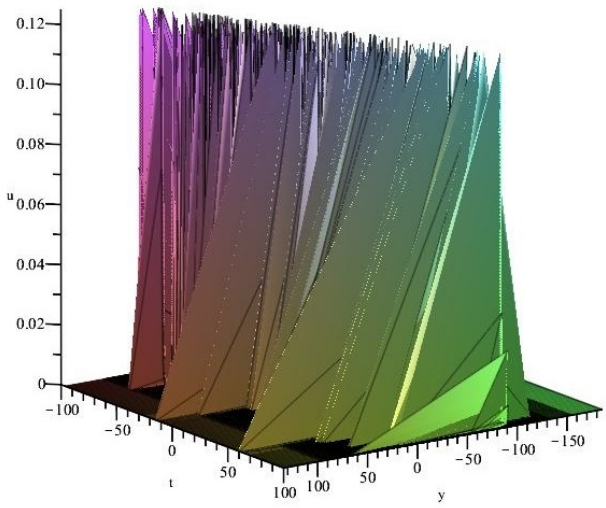

Fig. 36. Chaotic soliton solution $u(x, y, t)_{\text{Soliton}}$ for $x = 0$ by replacing y with $\theta(s)$

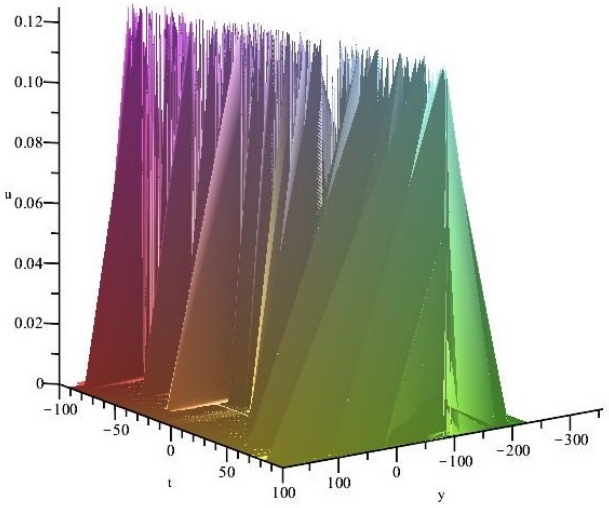

Fig. 38. Chaotic soliton solution $u(x, y, t)_{\text{Soliton}}$ for $x = 0$ by replacing y with $\phi(s)$.

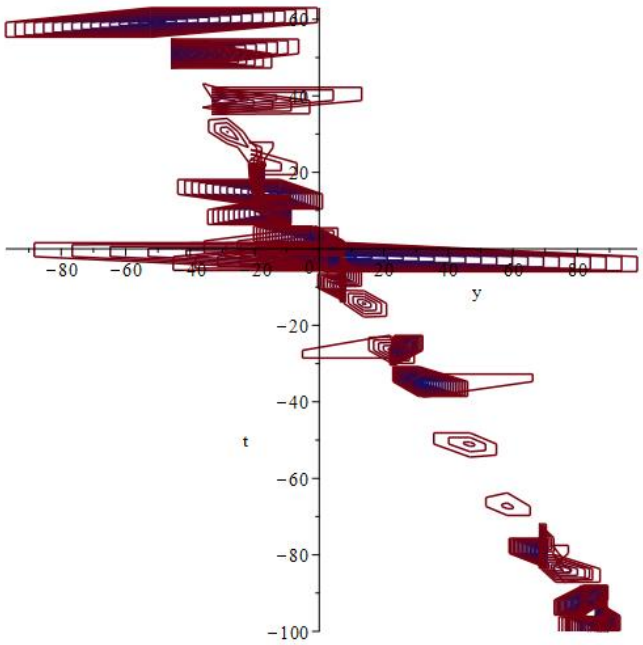

Fig. 37. Contour plot of chaotic soliton solution $u(x, y, t)_{\text{Soliton}}$ for $x = 0$ by replacing y with $\theta(s)$.

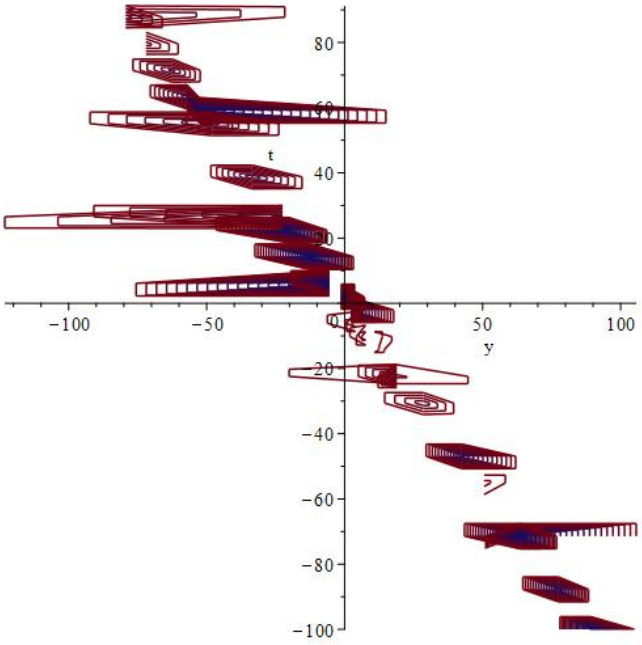

Fig. 39. Contour plot of chaotic soliton solution $u(x, y, t)_{\text{Soliton}}$ for $x = 0$ by replacing y with $\phi(s)$.

comparing Figure 1 with Figures 36 and 38), we can observe that the soliton solution exhibits distinct chaotic behavior.

Secondly, we substitute $\theta(s)$ and $\phi(s)$ for the variable x in the breather solution (11), and then illustrate the chaotic behavior of the resulting solution, as shown in Figures 40, 41, 42 and 43. Broadly speaking, these solutions retain a certain degree of periodicity while exhibiting distinct chaotic behavior—a trend that becomes more intuitive when compared with Figure 8.

Thirdly, we substitute $\theta(s)$ and $\phi(s)$ for the variable x in the lump solution (13), and use Maple software to plot the corresponding graphs, with details provided in Figures 44, 45, 46, 47, 48 and 49. From these figures, it is evident that, in contrast to the regularity of the original lump solution (Figure 17), the modified solutions exhibit highly pronounced chaotic behavior.

Finally, we substitute $\theta(s)$ and $\phi(s)$ for the variable x in the interaction solution (15) to obtain chaotic interaction solutions, whose graphs are presented in Figures 50, 51, 52 and 53. A comparison of the solution graphs before and after substitution reveals that the interaction solution transitions from its original regular periodicity (Figure 26) to a highly irregular chaotic state.

VII. Conclusions

In this paper, we conducted a comparative analysis of the Boussinesq and Kadomtsev-Petviashvili equations, identifying shared terms such as $(u^2)_{xx}$ and u_{xxxx}. We then integrated their distinctive characteristics to formulate the KPB equation, which carries clear physical significance—particularly the u_{tt} term, which reflects the evolutionary behavior of solutions. We derived and presented

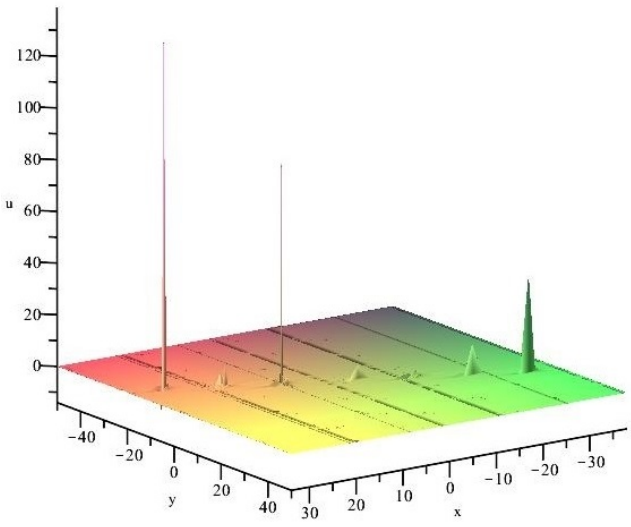

Fig. 40. Chaotic breather solution $u(x, y, t)_{\text{Breather}}$ for $t = 0$ by replacing x with $\theta(s)$.

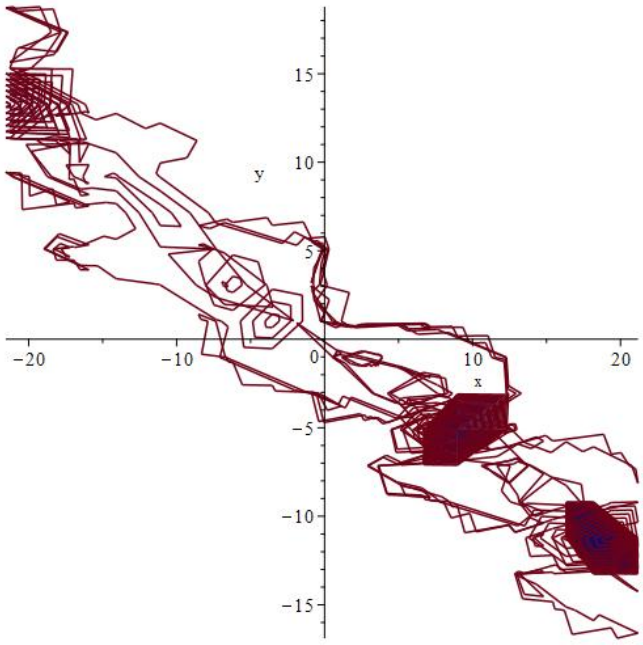

Fig. 41. Contour plot of chaotic breather solution $u(x, y, t)_{\text{Breather}}$ for $t = 0$ by replacing x with $\theta(s)$.

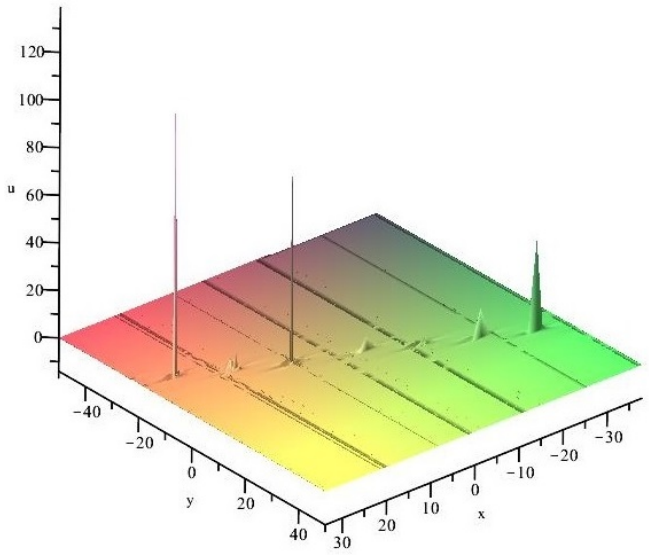

Fig. 42. Chaotic breather solution $u(x, y, t)_{\text{Breather}}$ for $t = 0$ by replacing x with $\phi(s)$.

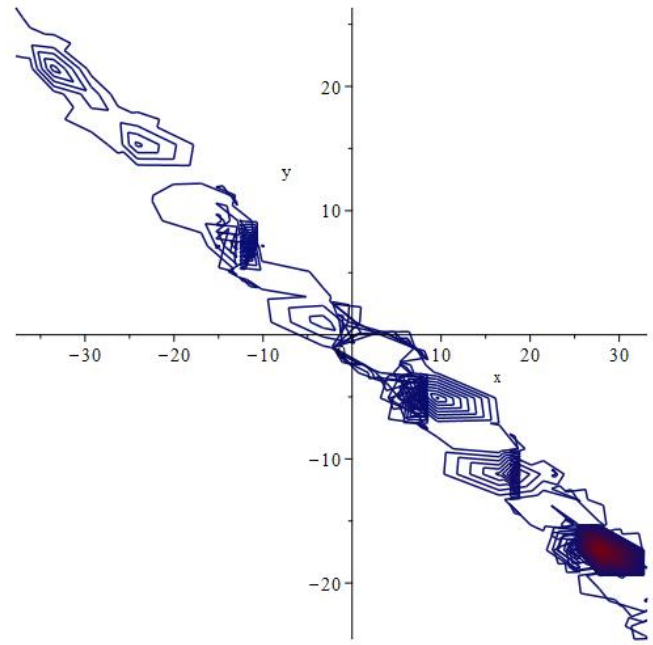

Fig. 43. Contour plot of chaotic breather solution $u(x, y, t)_{\text{Breather}}$ for $t = 0$ by replacing x with $\phi(s)$.

its 2D soliton, breather, lump, and interaction solutions, all of which exhibit practical application potential.

Theoretically, in the field of physics, the soliton solutions of the KPB equation reveal the intrinsic nature of nonlinear waves, with applications spanning fluid dynamics, quantum fields, and beyond. Breather solutions describe energy fluctuation phenomena in optics and plasma physics, thereby expanding the research scope of nonlinear dynamics. Lump solutions contribute to the understanding of material states, while interaction solutions play a pivotal role in atomic and quantum contexts, enabling the construction of complex multi-scale models. Mathematically, as an integrable system, the KPB equation enriches solution spaces, facilitates investigations into conservation laws, and advances the development of solution methodologies.

The incorporation of double pendulum chaos into the equation's solutions holds profound implications. Theoretically, it transcends the limitations of regular solutions, deepening our comprehension of the complexity of nonlinear waves and cross-model chaotic behaviors. Practically, it enhances applications across both micro and macro domains, such as optimizing soliton-based communication encryption, refining breather-simulated wave energy analysis, improving lump-based material modeling, and strengthening multi-scale interaction simulations using interaction solutions.

Our research demonstrates innovation by providing valuable references for chaos studies in PDEs, while also bearing significant practical value.

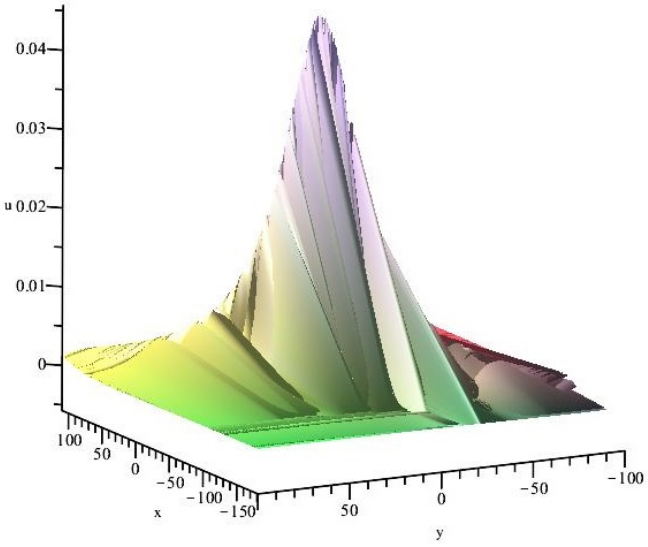

Fig. 44. 3D plot of the chaotic lump solution $u(x, y, t)_{\text{Lump}}$ for $t = 2$ by replacing x with $\theta(s)$.

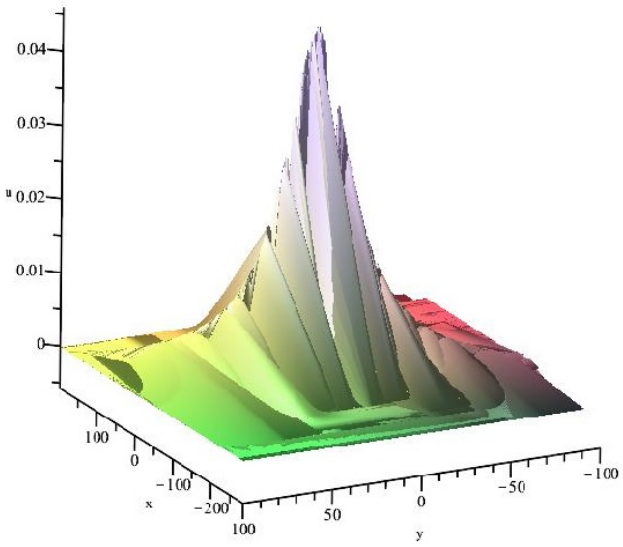

Fig. 47. 3D plot of the chaotic lump solution $u(x, y, t)_{\text{Lump}}$ for $t = 2$ by replacing x with $\phi(s)$.

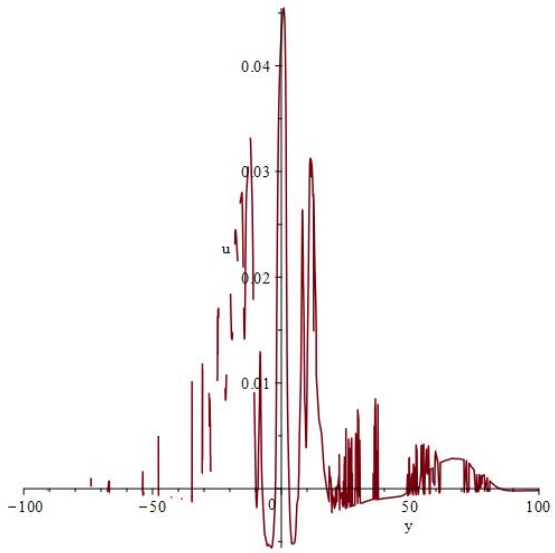

Fig. 45. 2D plot of the chaotic lump solution $u(x, y, t)_{\text{Lump}}$ for $t = 2$ by replacing x with $\theta(s)$.

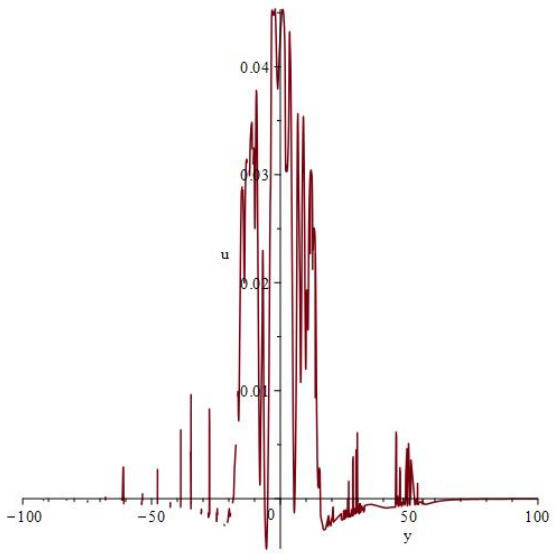

Fig. 48. 2D plot of the chaotic lump solution $u(x, y, t)_{\text{Lump}}$ for $t = 2$ by replacing x with $\phi(s)$.

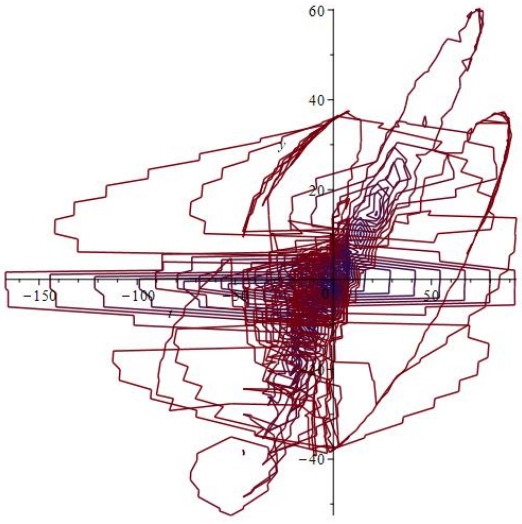

Fig. 46. Contour plot of the chaotic lump solution $u(x, y, t)_{\text{Lump}}$ for $t = 2$ by replacing x with $\theta(s)$.

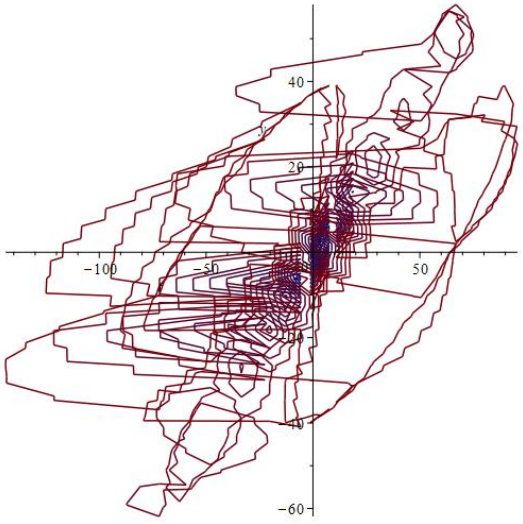

Fig. 49. Contour plot of the chaotic lump solution $u(x, y, t)_{\text{Lump}}$ for $t = 2$ by replacing x with $\phi(s)$.

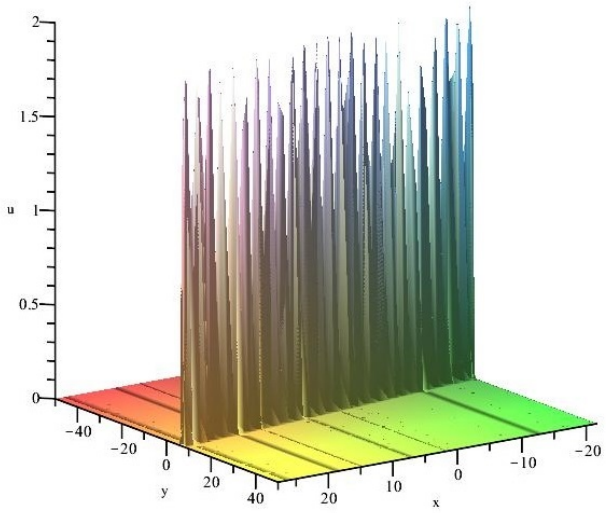

Fig. 50. Chaotic interaction solution $u(x, y, t)_{\text{Interaction}}$ for $t = 0$ by replacing x with $\theta(s)$.

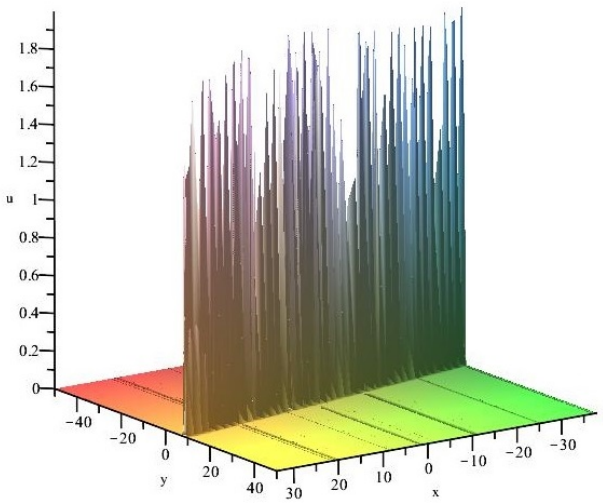

Fig. 52. Chaotic interaction solution $u(x, y, t)_{\text{Interaction}}$ for $t = 0$ by replacing x with $\phi(s)$.

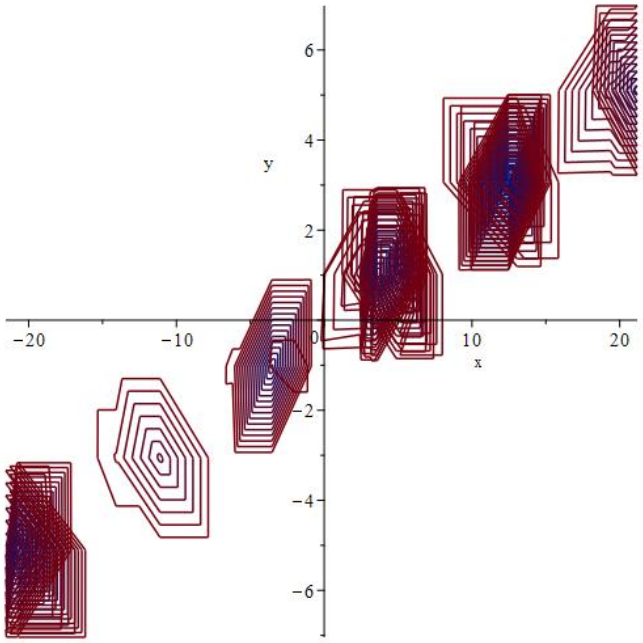

Fig. 51. Contour plot of chaotic interaction solution $u(x, y, t)_{\text{Interaction}}$ for $t = 0$ by replacing x with $\theta(s)$.

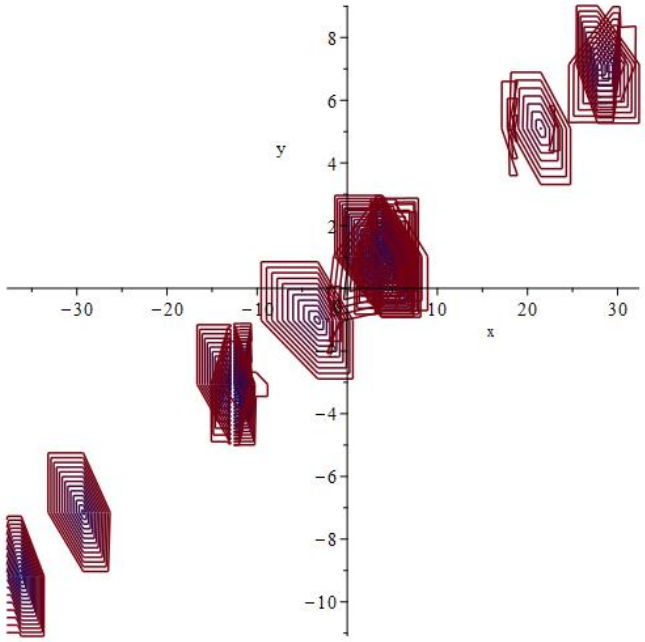

Fig. 53. Contour plot of chaotic interaction solution $u(x, y, t)_{\text{Interaction}}$ for $t = 0$ by replacing x with $\phi(s)$.

REFERENCES

[1] A. Asmaa, W. Zhang, T. S. Amer, and H. Li. "Nonlinear vibration analysis of a 3DOF double pendulum system near resonance," *Alexandria Engineering Journal*, *2025*, 113, pp. 262-286.

[2] A. T. Ali, B. Al-Khamaiseh, and A. H. Alkasasbeh. "New improvement of the ϕ^6-model expansion method and its applications to the new (3+1)-dimensional integrable Kadomtsev-Petviashvili equation," *Partial Differential Equations in Applied Mathematics*, *2024*, 11, 100883.

[3] C. Chai and K. J. Wang. "Non-singular complexiton, singular complexiton and the breather wave solutions to the (2+1)-dimensional Sawada-Kotera equation," *Results in Physics*, *2024*, 57, 107348.

[4] W. Chen, R. Guan, and L. Tian. "Interaction phenomenon and breather wave to the extend (3+1)-dimensional Kadomtsev-Petviashvili equation," *Journal of Mathematical Analysis and Applications*, *2023*, 518, 126650.

[5] W. Chen, L. Tang, L. Tian, and X. Yang. "Breather and multiwave solutions to an extended (3+1)-dimensional Jimbo-Miwa-like equation," *Applied Mathematics Letters*, *2023*, 145, 108785.

[6] M. K. Elboree. "Lump solitons, rogue wave solutions and lump-stripe interaction phenomena to an extended (3+1)-dimensional KP equation," *Chinese Journal of Physics*, *2020*, 63, pp. 290-303.

[7] U. Esma. "Travelling wave and optical soliton solutions of the Wick type stochastic NLSE with conformable derivatives," *Chaos, Solitons and Fractals*, *2021*, 148, 111052.

[8] J. Fang, D. Mou, Y. Wang, and others. "Soliton dynamics based on exact solutions of conformable fractional discrete complex cubic Ginzburg Landau equation," *Results in Physics*, *2021*, 20, 103710.

[9] Y. Gu, L. Peng, Z. Huang, and Y. Lai. "Soliton, breather, lump, interaction solutions and chaotic behavior for the (2+1)-dimensional KPSKR equation," *Chaos, Solitons and Fractals*, *2024*, 187, 11535.

[10] Y. Gu, J. Manafian, S. Malmir, B. Eslami, and O. A. Ilhan. "Lump, lump-trigonometric, breather waves, periodic wave and multiwaves solutions for a Konopelchenko-Dubrovsky equation arising in fluid dynamics," *International Journal of Modern Physics B*, *2023*, 2350141, DOI: 10.1142/S0217979223501412.

[11] J. Hietarinta. "Introduction to the Hirota bilinear method," arXiv:solv-int/9708006v1, 14 Aug, *1997*.

[12] M. Hijazi, M. S. Ajeel, K. Al-Khaled, H. Al-Khalid. "Perturbation Methods for Solving Non-Linear Ordinary Differential Equations,"

IAENG International Journal of Applied Mathematics, 2024, vol. 54, no. 10, pp2070-2082.

[13] R. Hirota. "The direct method in soliton theory," *Cambridge University Press*, *2004*.

[14] K. Hosseini, E. Hincal, K. Sadri, F. Rabiei, M. Ilie, A. Akgül, and M. S. Osman. "The positive multi-complexiton solution to a generalized Kadomtsev-Petviashvili equation," *Partial Differential Equations in Applied Mathematics*, *2024*, 9, 100647.

[15] D. Igobi, W. Udogworen. "Results on Existence and Uniqueness of solutions of Fractional Differential Equations of Caputo-Fabrizio type in the sense of Riemann-Liouville," *IAENG International Journal of Applied Mathematics*, 2024, vol. 54, no. 6, pp1163-1171.

[16] Z. Z. Lan. "N-soliton solutions, Bäcklund transformation and Lax Pair for a generalized variable-coefficient cylindrical Kadomtsev-Petviashvili equation," *Applied Mathematics Letters*, *2024*, 158, 109239.

[17] F. Li, Y. Qian, and S. Wu. "A self-adapting trajectory tracking control for double-pendulum marine tower crane considering constraint dead zone against seawave disturbances," *Ocean Engineering*, *2024*, 309, Part 1, 118358.

[18] J. Li and G. Chen, and Y. Zhou. "Bifurcations and exact traveling wave solutions of two shallow water two-component systems," *International Journal of Bifurcation and Chaos*, *2021*, 31(1), 2150001.

[19] J. G. Liu. "Lump-type solutions and interaction solutions for the (2+1)-dimensional generalized fifth-order KdV equation," *Applied Mathematics Letters*, *2018*, 86, pp. 36-41.

[20] J. G. Liu. "Double-periodic soliton solutions for the (3+1)-dimensional Boiti-Leon-Manna-Pempinelli equation in incompressible fluid," *Computers and Mathematics with Applications*, *2018*, 75(10), pp. 3604-3613.

[21] J. Luo. "Dynamical behavior analysis and soliton solutions of the generalized Whitham-Broer-Kaup-Boussineq-Kupershmidt equations," *Results in Physics*, *2024*, 60, 10766.

[22] H. Ma, X. Mao, and A. Deng. "Interaction solutions for the second extended (3+1)-dimensional Jimbo-Miwa equation," *Chinese Physics B*, *2023*, 32, 060201.

[23] H. Ma, X. Chen, and A. Deng. "Novel soliton molecule solutions for the second extend (3+1)-dimensional Jimbo-Miwa equation in fluid mechanics," *Communications in Theoretical Physics*, *2023*, 75, 125004.

[24] W. X. Ma. "Soliton solutions by means of Hirota bilinear form," *Partial Differential Equations in Applied Mathematics*, *2022*, 5, 100220.

[25] W. X. Ma. "Type λ^*, λ reduced nonlocal integrable AKNS equations and their soliton solutions," *Applied Numerical Mathematics*, *2024*, 199, pp. 105-113.

[26] W. X. Ma and Y. Zhou. "Lump solutions to nonlinear partial differential equations via Hirota bilinear forms," *Journal of Differential Equations*, *2018*, 264(4), pp. 2633-2659.

[27] V. Mahé, A. Grolet, A. Renault, H. Mahé, and O. Thomas. "Dynamic stability and efficiency of centrifugal double pendulum vibration absorbers," *Mechanism and Machine Theory*, *2024*, 197, 105649.

[28] J. Manafian. "Novel solitary wave solutions for the (3+1)-dimensional extended Jimbo-Miwa equations," *Computers and Mathematics with Applications*, *2018*, 76, pp. 1246-1260.

[29] M. Wei, F. Fan, and X. Chen. "Existence of periodic and solitary waves of a Boussinesq equation under perturbations," *Nonlinear Analysis: Real World Applications*, *2025*, 81, 104223.

[30] B. Qin and Y. Zhang. "A novel global perspective: Characterizing the fractal basins of attraction and the level of chaos in a double pendulum," *Chaos, Solitons and Fractals*, *2024*, 189, Part 1, 115694.

[31] H. Sun and A. H. Chen. "Lump and lump-kink solutions of the (3 + 1)-dimensional Jimbo-Miwa and two extended Jimbo-Miwa equations," *Applied Mathematics Letters*, *2017*, 68, pp. 55-61.

[32] S. F. Tian. "Lie symmetry analysis, conservation laws and solitary wave solutions to a fourth-order nonlinear generalized Boussinesq water wave equation," *Applied Mathematics Letters*, *2020*, 100, 106056.

[33] A. M. Wazwaz. "Study on a (3+1)-dimensional B-type Kadomtsev Petviashvili equation in nonlinear physics: Multiple soliton solutions, lump solutions, and breather wave solutions," *Chaos, Solitons and Fractals*, *2024*, 189, Part 1, 115668.

[34] Y. Xu, X. Geng, and Y. Zhai. "Riemann theta function solutions to the semi-discrete Boussinesq equations," *Physica D: Nonlinear Phenomena*, *2024*, 470, Part A, 134398.

[35] J. Y. Yang, W. X. Ma, and Z. Y. Qin. "Lump and lump-soliton solutions to the (2+1)-dimensional Ito equation," *Analysis and Mathematical Physics*, *2018*, 8, pp. 427-436.

[36] X. Yang, L. Tang, X. Gu, W. Chen, and L. Tian. "Lump and interaction solutions to a (3+1)-dimensional BKP-Boussinesq-like equation," *Journal of Mathematical Analysis and Applications*, *2025*, 543, Issue 2, Part 3, 129030.

[37] Z. Yan, Y. Yan, M. Liu, and W. Liu. "Propagation properties of bright solitons generated by the complex Ginzburg-Landau equation with high order dispersion and nonlinear gradient terms," *Applied Mathematics Letters*, *2024*, 157, 109164.

[38] A. Zafar, M. Ijaz, M. E. Sayed, and others. "Exploring the fractional Hirota-Maccari system for its soliton solutions via impressive analytical strategies," *Results in Physics*, *2022*, 43, 106049.

[39] H. Q. Zhang and W. X. Ma. "Lump solutions to the (2+1)-dimensional Sawada-Kotera equation," *Nonlinear Dynamics*, *2017*, 87, pp. 2305-2310.

[40] J. B. Zhang and W. X. Ma. "Mixed lump-kink solutions to the BKP equation," *Computers and Mathematics With Applications*, *2017*, 74(3), pp. 591-596.

[41] J. Zhang and J. Huang. "Convergence rates and central limit theorem for 3-D stochastic fractional Boussinesq equations with transport noise," *Physica D: Nonlinear Phenomena*, *2024*, 470, Part A, 134406.

[42] X. Zhang, X. Li, and G. Ma. "Optical soliton noninteraction transmission in optical communication systems," *Applied Mathematics Letters*, *2025*, 162, 109383.

[43] X. Zhang, L. Wang, W. Q. Chen, X. M. Yao, X. Wang, and Y. C. Zhao. "Dynamics of transformed nonlinear waves in the (3 + 1)-dimensional B-type Kadomtsev-Petviashvili equation I: Transitions mechanisms," *Communications in Nonlinear Science and Numerical Simulation*, *2022*, 105, 106070.

[44] X. H. Zhao. "Multi-solitons and integrability for a (2 + 1)-dimensional variable coefficients Date-Jimbo-Kashiwara-Miwa equation," *Applied Mathematics Letters*, *2024*, 149, 108895.

[45] M. Horbatsch. "Computational Physics using Maple," URL: https://www.yorku.ca/marko/ComPhys/, *2003*.